



Direct fabrication of a q -plate array by scanning wave photopolymerization

MIHO AIZAWA,^{1,2} MEGUMI OTA,^{1,2} KYOHEI HISANO,^{1,3} NORIHISA AKAMATSU,^{1,2} TAKEO SASAKI,⁴ CHRISTOPHER J. BARRETT,^{1,5} AND ATSUSHI SHISHIDO^{1,2,*}

¹Laboratory for Chemistry and Life Science, Institute of Innovative Research, Tokyo Institute of Technology, R1-12, 4259 Nagatsuta, Midori-ku, Yokohama 226-8503, Japan

²Department of Chemical Science and Engineering, School of Materials and Chemical Technology, Tokyo Institute of Technology, 2-12-1 Ookayama, Meguro-ku, Tokyo 152-8552, Japan

³Department of Applied Chemistry, College of Life Sciences, Ritsumeikan University, 1-1-1 Nojihigashi, Kusatsu 525-8577, Japan

⁴Department of Chemistry, Faculty of Science, Tokyo University of Science, 1-3 Kagurazaka Shinjuku-ku, Tokyo 162-8601, Japan

⁵Department of Chemistry, McGill University, 801 Sherbrooke St. W., Montreal, Québec H3A 0B8, Canada

*Corresponding author: ashishid@res.titech.ac.jp

Received 18 December 2018; accepted 10 January 2019; posted 14 January 2019 (Doc. ID 353341); published 19 February 2019

Topological lightwave technologies are expected to be applied in a wide range of emerging optical fields such as q -plates, one of the most attractive devices in this research area, prepared by controlling the high-resolution alignment patterning of liquid crystals. Here, we present a simple and direct fabrication technique of a q -plate that is able to oscillate a vector beam, by employing our newly developed photoalignment concept termed scanning wave photopolymerization (SWaP). SWaP generates precise arbitrary molecular alignment patterns concurrent with irradiated light patterns, successfully fabricating a polymer film with a radial molecular alignment arranged in an array pattern in a single step. This array patterned alignment structure was able to simultaneously generate a vector beam, indicating that SWaP can be utilized for producing such topological lightwave applications. © 2019 Optical Society of America

<https://doi.org/10.1364/JOSAB.36.000D47>

1. INTRODUCTION

Manipulation of polarization, intensity, and shape of a laser beam is a key technology for various optical device applications. In recent years, the availability of topological lightwaves with an orbital angular momentum has gained prominence in various fields such as nano-materials fabrication and biomedical optical devices in the life sciences [1,2]. Topological lightwaves can be classified as an optical vortex of a helically phased beam and a vector beam with a spatial distribution of polarization, created by the precise control of topological structures of the phase fronts and polarization. By applying the specific properties of these optical vortex and vector beams, many applications have been proposed, such as material processing with laser irradiation [3], optical tweezers [4], super-resolution microscopes [5–7], and free-space communication [8]. From the first discovery of orbital angular momentum control of the topological waves reported in 1992 [9], research into topological lightwaves has developed dramatically [10]. In particular, a waveplate with a specific optical function to convert a phase polarization state of a laser beam into optical axis symmetry is now one of the most desired and useful devices in this field [11,12]. Q -plates function as optical devices that can generate light beams with orbital angular momentum of light, from a

beam with well-defined spin angular momentum of light, based on spin-orbit momentum coupling that may occur in a medium that is both anisotropic and inhomogeneous, with a sign controlled by the input polarization. Practically, a q -plate can be fabricated simply as a birefringent waveplate with a two-dimensional (2D) patterned distribution of the optical axis in the transverse plane, and “ q ” denotes a semi-integer topological charge defined as the degree of optical axis distribution. For example, it is known that a film having a π rotated optical axis of the retardation rotated on a laser optical axis works as a $q = 1$ q -plate. The result is a radial vector beam or an optical vortex obtained when linearly polarized light or circularly polarized light is introduced to the film, respectively.

Liquid crystals (LCs) are now attractive as a powerful material to prepare these q -plates [13–15]. For example, a LC can show large anisotropy in a refractive index due to its shape anisotropy. In addition, molecular motion and alignment states of LCs can propagate over long distances by cooperative molecular effects; thus, a spatial optical axis could be defined by external stimuli [16]. For controlling the alignment behavior of LCs, various photoalignment methods have been developed [17–20]. In these photoalignment processes, molecular alignment is generated by the exposure of linearly polarized light to

LC materials containing photoresponsive dye molecules such as azobenzene or cinnamic acid derivatives [21]. Thus, arbitrary 2D alignment patterns have been achieved by inducing a spatial distribution of polarization states using a spatial light modulator (SLM) or an interference irradiation of polarized light [22–25]. In particular, photoirradiation using a SLM can realize the complex alignment patterns with high spatial resolution [26–28]. However, an irradiation pattern with light divided into a large number of pixels is required to form complex alignment patterns such as radial alignment, in order to obtain a film performing as a q -plate, because the molecular alignment can be generated in just one direction at each time exposure. Therefore, it was previously impossible to fabricate a film with minute structures approaching the diffraction limit of the light used, over the multiple processes required. Moreover, enormous time and cost would be needed to form complicated and macroscopically aligned structures such as an array pattern.

Recently, we reported the development of a new concept in photoalignment processes, based on scanning wave photopolymerization (SWaP), which enables one to generate microscopic alignment array patterns easily and cheaply over large areas [29–31]. With SWaP, the spatiotemporal control of the irradiated light during photopolymerization generates arbitrary alignment patterns in the LC, because molecular alignment is induced by a mass flow arising from the difference in chemical potential at the propagating reaction wavefront. Thus, this new process has some great advantages in terms of processability of array patterns having alignment with a resolution that reaches the diffraction limit in a single step, so it is an ideal candidate process for q -plate inscription. In this present work, we report the successful generation of vector beams from an inscribed q -plate with a radial alignment array pattern over a large area fabricated by SWaP. The processing times for the array patterns was several minutes, but the resolution of the resultant aligned structures achievable was significantly improved over those prepared by conventional photoalignment processes, and the number of the possible arrays produced was also drastically increased. Furthermore, analysis revealed that a linearly polarized light beam was successfully converted to a vector beam by the q -plate fabricated, optimized by the retardation of the film. The large area q -plate arrays potentially patternable with microscale patterned structures formed by SWaP can be reasonably expected to significantly expand the range of potential applications of vector beams.

2. DESIGN AND FABRICATION

To fabricate a q -plate with fine molecular alignment patterns, SWaP was conducted using a digital light processor (DLP), which can precisely control the shape and movement of the irradiation light. The DLP is equipped with a digital micromirror device (DMD) with a 1280×720 array of mirrors, and UV-LED ($\lambda_{\max} = 372$ nm) was used as the UV light source, and this device was combined with a polarized optical microscope (POM). The size of each pixel was determined by observation with a beam profiler and was found to be $3.45 \mu\text{m}$ with a $\times 4$ objective lens. The irradiation light pattern was designed using software (Adobe Illustrator). The $3 \mu\text{m}$ thick glass cells used for the photopolymerization process were handmade by

adhering cleaned glass substrates, which were $25 \text{ mm} \times 25 \text{ mm}$ glass and a $18 \text{ mm} \times 18 \text{ mm}$ microscope coverslip glass, with glue separated by $2\text{--}5 \mu\text{m}$ thick silica bead spacers. A photopolymerizable sample mixture was composed of 6-(4-cyano-4'-biphenyloxy) hexyl acrylate (A6CB), hexanediol dimethacrylate (HDDMA, Waco Chemical) and a photoinitiator Irgacure 651 (Ciba Specialty Chemicals), with a composition ratio for this sample the same as described in a previous paper [30]. The sample was injected into a prepared glass cell by capillary force at 150°C , the isotropic temperature of this sample. After cooling the glass cell to 100°C , photopolymerization with patterned light at an intensity of $1.2 \text{ mW}/\text{cm}^2$ was carried out. Following the photoirradiation of the whole area with $5.0 \text{ mW}/\text{cm}^2$ intensity UV light for fixing the generated molecular alignment, the sample cell was rapidly cooled down below its glass transition temperature with liquid nitrogen.

3. RESULTS AND DISCUSSION

Photopolymerization patterning was conducted with an optical image of a hexagonal lattice with a size of $300 \mu\text{m} \times 300 \mu\text{m}$ and an irradiated region width of $31 \mu\text{m}$ to generate a large area alignment array pattern [Fig. 1(a)]. The exposure time was 4 min to complete photopolymerization. As shown in Fig. 1(b), observation with a POM of the fabricated film revealed that a periodic pattern of optical anisotropy was induced over the whole area, with the periodicity of the contrast depending on the irradiated hexagonal pattern. Note that the center of the lattice remained dark, independent of the rotation angle of the film. Figure 1(c) shows the POM image with a test plate with a retardation of 137 nm . An additive effect was observed only in the lower left and upper right regions of the hexagonal pattern. Moreover, the size of each alignment structure was $294 \mu\text{m} \times 294 \mu\text{m}$, which is almost the same period as the hexagonal lattice of the irradiated pattern. These results indicate that radial molecular alignment with a topological defect of

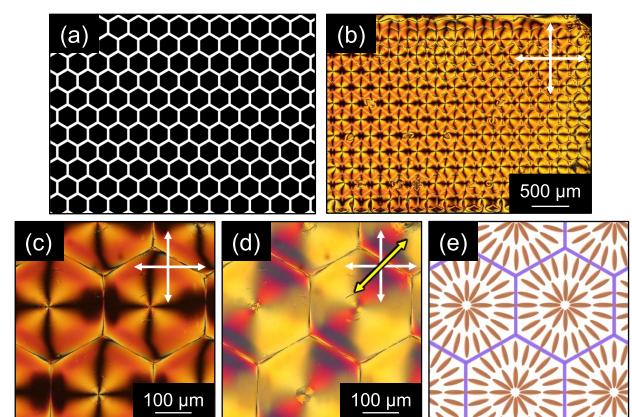


Fig. 1. (a) Optical pattern of a hexagonal lattice. White lines represent the irradiated regions. (b)–(d) Polarized optical micrographs of the resultant polymer film under crossed polarizers (b), (c) without a test plate and (d) with a test plate having a retardation of 137 nm , respectively. (e) Schematic illustration of the resultant molecular alignment pattern generated from the photoirradiation with the optical pattern. Blue lines define the irradiated region, and orange ellipses indicate the long axis direction of molecules.

$q = +1$ was generated in each hexagonal lattice pattern, as illustrated in Fig. 1(d), and that the alignment structures were arranged into an array pattern coincident with the pattern of the incident light. In SWaP, the driving force for generating molecular alignment during photopolymerization is molecular diffusion along a light intensity gradient; thus, the irradiation of the hexagonal array pattern leads to the induction of the radial alignment. The resultant film has approximately 200 patterns of radial alignment in the irradiated region, with a size of $300\ \mu\text{m}$. This suggests that SWaP is more advantageous than conventional photoalignment techniques in terms of the number and the size of array patterns achievable. Furthermore, the net processing time was drastically reduced because the complex array patterns can be generated in a single step via SWaP.

To investigate whether the polymer film with radial alignment patterns formed by SWaP could perform effectively as a q -plate, we examined the optical functionality of the film using a He–Ne laser with a wavelength of $633\ \text{nm}$. For a q -plate, it is important to optimize the retardation to the half-waveplate condition at the wavelength of an incident beam, to function as a vector–vortex waveplate. Thus, retardation of the photopolymerized film with a radial molecular alignment pattern was observed with a Berek compensator. The value was found to be $326\ \text{nm}$, which is almost the same as the half-wavelength of the $633\ \text{nm}$ input beam. We used a laser beam equipped with a polarizer as an incident light beam, detected with a beam profiler, and it was confirmed that the light had a Gaussian distribution profile with a beam diameter of $160\ \mu\text{m}$ [Fig. 2(a)]. When a He–Ne laser beam with vertical polarization was incident on the resultant film with a retardation of $326\ \text{nm}$, the transmitted light was transformed to a doughnut beam, as shown in Fig. 2(b). We performed analysis of the light intensity distribution of the transmitted light by using image analysis software (Image J). As a result, the light intensity at

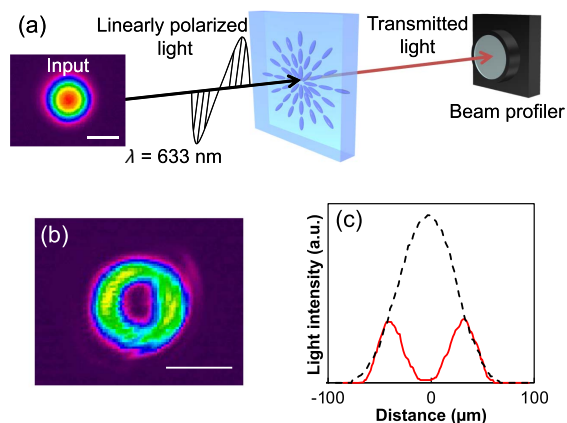


Fig. 2. (a) Schematic illustration of the optical setup for evaluation of optical properties where a linearly polarized He–Ne laser beam propagated. The inset shows the 2D intensity profile of an incident He–Ne laser beam with a Gaussian distribution. (b) Beam profile and (c) one-dimensional (1D) intensity profiles of a He–Ne laser beam that propagated through the resultant polymer film with radial alignment. In 1D profiles, red and black broken lines depict the 1D profile of the transmitted, and of incident laser beams, respectively. The scale bar = $100\ \mu\text{m}$.

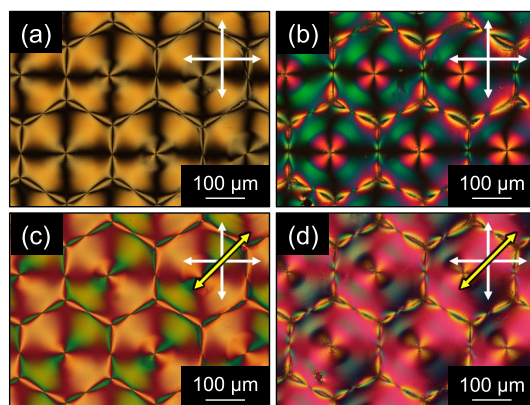


Fig. 3. Polarized optical micrographs of a film with (a), (c) $R = 196\ \text{nm}$, and (b), (d) $R = 400\ \text{nm}$. Polarized optical micrographs of resultant polymer films under crossed polarizers either without (a), (b), or with (c), (d) a test plate with a retardation of $530\ \text{nm}$. White arrows show the direction of polarizers. Yellow arrows indicate the optical axis of the test plate.

the center of the transmitted light decreased to $\sim 3\%$ of its original intensity, as shown in Fig. 2(c).

Next, we examined the effect of retardation of the film fabricated by SWaP on the generation of a vector beam. Based on the consideration that retardation depends on the birefringence and film thickness, and that the birefringence of the polymer film prepared by SWaP is in the range of 0.08 – 0.15 according to the previous study [30], SWaP was performed in glass cells with different cell thicknesses. Investigation of the film with a POM indicated that periodic changes of molecular alignment were generated in the films, as shown in Figs. 3(a) and 3(b). As described above, POM observation with a test plate showed that the alignment direction was radially rotated along the hexagonal pattern, as shown in Figs. 3(c) and 3(d). Therefore, it was confirmed that the radial molecular alignment accumulated into the array formed was also induced by the irradiation of an

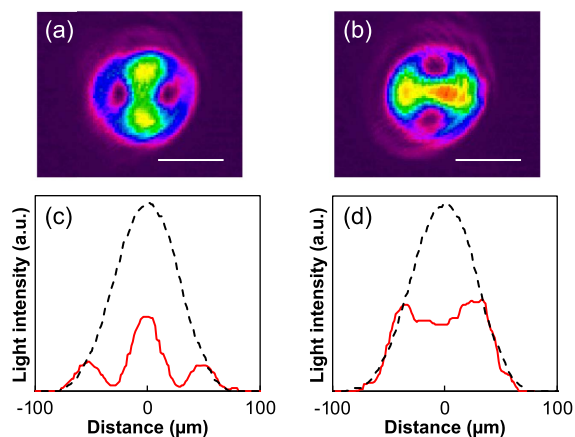


Fig. 4. (a), (b) Measured beam shape through a film with $R = 196\ \text{nm}$ and $R = 400\ \text{nm}$, respectively. Scale bar = $100\ \mu\text{m}$. (c), (d) One-dimensional intensity profiles of the incident laser beam (black broken line), and transmitted light through a film with $R = 196\ \text{nm}$ and $R = 400\ \text{nm}$, respectively (red line).

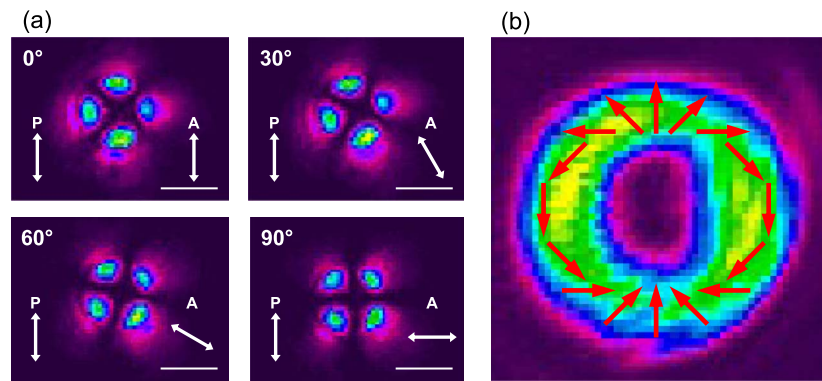


Fig. 5. (a) Beam profile of a film with $R = 326$ nm observed through an analyzer. (b) Optical axis distribution of the doughnut beam detected. Scale bar = 100 μm .

optical pattern with a hexagonal array despite a difference in cell thickness. Retardation values of these films were determined with a Berek compensator to be 196 nm and 400 nm, respectively. Figure 4 shows the beam profile of the light through the resultant polymer films when a vertically polarized He–Ne laser beam was incident on the films. These photographs indicate that both transmitted beams were not transformed into doughnut-like beams, although the films had a radial molecular alignment pattern. To make the films function as a generation device of a vector beam, it is essential that the retardation meets half-waveplate conditions for the input beam in order to convert the linearly polarized light with different directions for induction of interference of laser beams. When linearly polarized light was input to the film with retardation values of 196 nm or 400 nm, which do not match the half-waveplate condition for 633 nm, the transmitted light beam profile was converted to an elliptical polarization. Therefore, the beam profile became a distorted shape. SWaP thus enables one to produce a q -plate that can perform with various wavelengths simply by controlling the cell thickness.

A beam propagated through the film with radial alignment retardation of 326 nm was analyzed by observing the transmitted light using a polarizer inserted in front of the beam profiler to investigate whether the beam was converted to a vector beam. By introducing an analyzer, the polarization distribution of the doughnut beam emerging from the polymer film was examined. Figure 5(a) reveals that the doughnut ring was divided into four separated beams. As the analyzer was rotated, the 2D intensity profile of the output beam was rotated, keeping four symmetrical bright spots. This observation suggests that the polarization direction of the doughnut profile was rotated relative to the radially molecular alignment direction, as shown in Fig. 5(b). When the polarization direction was parallel to the molecular alignment direction, the polarization state remained unchanged, but when the angle θ formed was non-zero, the resultant polarization was rotated by 2θ . Therefore, it was clear that the propagated doughnut beam passing through a film with a radial alignment pattern fabricated by SWaP was converted to the polarized vector beam with a rotating polarization vector of 4π around the defect. It is reasonable to assume that the vector beam, with the polarization vector rotated by the

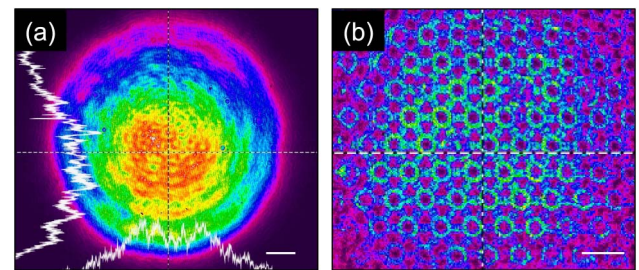


Fig. 6. (a) Beam profile of the incident light and (b) transmitted light through the polymer film with array patterns. Scale bar = 500 μm .

double period of the q -plate, was produced because the alignment direction of LC molecules was rotated by 2π in the radial alignment pattern, and linearly polarized light was converted symmetrically on the optical axis by a half-waveplate condition. On the other hand, in the case of the films that do not meet the half-waveplate condition for 633 nm, the transmitted component through the analyzer was detected, and the beam shape was observed to be distorted.

Simultaneous generation of the vector beams was explored using a film having a retardation of 326 nm, which meets the half-waveplate condition, by introducing an incident He–Ne laser beam, expanded to 4 mm as shown in Fig. 6(a). As a result, the light propagating through the polymer film with periodic radial alignment patterns showed that doughnut patterns were arranged in an array [Fig. 6(b)], with more than 50 such doughnut rings detected in the irradiated region simultaneously, proving that a polymer film that can simultaneously generate vector beams has been successfully fabricated over large areas in a single step.

4. CONCLUSION

In conclusion, we have demonstrated that a newly developed single-step photoalignment patterning technology (SWaP) enabled a highly efficient fabrication of a q -plate. By controlling the spatial parameters of irradiation light, such as the shape and the spatial movement, radial molecular alignment patterns

periodically arranged in an array could be generated over large areas in a single step, a demonstration difficult to achieve via conventional photoalignment methods. The resultant film with a radial molecular alignment pattern functioned successfully as a q -plate, generating a vector beam when the half-waveplate condition was met, based on control of retardation of the polymer film. SWaP thus has a great potential for fabricating q -plates and various other similar optical elements. Moreover, the fabricated q -plate film could be electrically switchable simply by adding a small amount of regular LCs. SWaP thus provides a new and powerful pathway for the simple creation of a variety of high-performance optical devices from displays to optical communication and super-resolution microscopy.

Funding. Core Research for Evolutional Science and Technology (CREST) (JPMJCR18I4); Japan Society for the Promotion of Science (JSPS) (JP18H05984, JP18J15144, JP18K14297, JP17H05250, JP18H05422).

Acknowledgment. This work was supported by JSPS KAKENHI grant no. JP17H05250 in Scientific Research on Innovative Areas “Photosynergetics” and JSPS KAKENHI grant no. JP18H05422 in Scientific Research on Innovative Areas “Molecular Engine: Design of Autonomous Functions through Energy Conversion.” This work was performed under the Cooperative Research Program of “NJRC Mater. & Dev.” This work was performed under the Research Program for CORE lab and Next Generation Young Scientists of “Five-star Alliance” in “NJRC Mater. & Dev.” The Tokyo Institute of Technology is thanked for sabbatical visit funding for Barrett in 2017 to the Shishido Labs, as Visiting Adjunct Professor.

REFERENCES

- Q. Zhan, “Cylindrical vector beams: from mathematical concepts to applications,” *Adv. Opt. Photon.* **1**, 1–57 (2009).
- A. M. Yao and M. J. Padgett, “Orbital angular momentum: origins, behavior and applications,” *Adv. Opt. Photon.* **3**, 161–204 (2011).
- M. Meier, V. Romano, and T. Feurer, “Material processing with pulsed radially and azimuthally polarized laser radiation,” *Appl. Phys. A* **86**, 329–334 (2007).
- D. G. Grier, “A revolution in optical manipulation,” *Nature* **424**, 810–816 (2003).
- S. W. Hell and J. Wichmann, “Breaking the diffraction resolution limit by stimulated emission: stimulated-emission-depletion fluorescence microscopy,” *Opt. Lett.* **19**, 780–782 (1994).
- B. Harke, J. Keller, C. K. Ullal, V. Westphal, A. Schönle, and S. W. Hell, “Resolution scaling in STED microscopy,” *Opt. Express* **16**, 4154–4162 (2008).
- Y. Kozawa, T. Hibi, A. Sato, H. Horanai, M. Kurihara, N. Hashimoto, H. Yokoyama, T. Nemoto, and S. Sato, “Lateral resolution enhancement of laser scanning microscopy by a higher-order radially polarized mode beam,” *Opt. Express* **19**, 15947–15954 (2011).
- J. Wang, J. Y. Yang, I. M. Fazal, N. Ahmed, Y. Yan, H. Huang, Y. Ren, Y. Yue, S. Dolinar, M. Tur, and A. E. Willner, “Terabit free-space data transmission employing orbital angular momentum multiplexing,” *Nat. Photonics* **6**, 488–496 (2012).
- L. Allen, M. W. Beijersbergen, R. J. C. Spreeuw, and J. P. Woerdman, “Orbital angular momentum of light and the transformation of Laguerre-Gaussian laser modes,” *Phys. Rev. A* **45**, 8185–8189 (1992).
- S. F. Arnold, L. Allen, and M. Padgett, “Advances in optical angular momentum,” *Laser Photon. Rev.* **2**, 299–313 (2008).
- L. Marrucci, C. Manzo, and D. Paparo, “Optical spin-to-orbital angular momentum conversion in inhomogeneous anisotropic media,” *Phys. Rev. Lett.* **96**, 163905 (2006).
- S. Slussarenko, A. Murauski, T. Du, V. Chigrinov, L. Marrucci, and E. Santamato, “Tunable liquid crystal q-plates with arbitrary topological charge,” *Opt. Express* **19**, 4085–4090 (2011).
- S. Nersisyan, N. Tabiryan, D. M. Steeves, and B. R. Kimball, “Fabrication of liquid crystal polymer axial waveplates for UV-IR wavelength,” *Opt. Express* **17**, 11926–11934 (2009).
- W. Ji, C. H. Lee, P. Chen, W. Hu, Y. Ming, L. Zhang, T. H. Lin, V. Chigrinov, and Y. Q. Lu, “Meta-q-plate for complex beam shaping,” *Sci. Rep.* **6**, 25528 (2016).
- S. V. Serak, D. E. Roberts, J. Y. Hwang, S. R. Nersisyan, N. V. Tabiryan, T. J. Bunning, D. M. Steeves, and B. R. Kimball, “Diffractive waveplate arrays,” *J. Opt. Soc. Am. B* **34**, B56–B63 (2017).
- T. Kato, J. Uchida, T. Ichikawa, and T. Sakamoto, “Functional liquid crystals towards the next generation of materials,” *Angew. Chem. Int. Ed.* **57**, 4355–4371 (2018).
- V. G. Chigrinov, V. M. Kozenkov, and H. S. Kwok, *Photoalignment of Liquid Crystalline Materials: Physics and Applications* (Wiley, 2008).
- O. Yaroshchuk and Y. Reznikov, “Photoalignment of liquid crystals: basics and current trends,” *J. Mater. Chem.* **22**, 286–300 (2012).
- A. Priimagi, C. J. Barrett, and A. Shishido, “Recent twists in photoactuation and photoalignment control,” *J. Mater. Chem. C* **2**, 7155–7162 (2014).
- T. Seki, “A wide array of photoinduced motions in molecular and macromolecular assemblies at interfaces,” *Bull. Chem. Soc. Jpn.* **91**(7), 1026–1057 (2018).
- T. Seki, S. Nagano, and M. Hara, “Versatility of photoalignment techniques: from nematics to a wide range of functional materials,” *Polymer* **54**, 6053–6072 (2013).
- G. P. Crawford, J. N. Eakin, M. D. Radcliffe, A. C. Jones, and R. A. Pelcovits, “Liquid-crystal diffraction gratings using polarization holography alignment techniques,” *J. Appl. Phys.* **98**, 123102 (2005).
- H. Wu, W. Hu, H. Hu, X. Lin, G. Zhu, J. W. Choi, V. Chigrinov, and Y. Lu, “Arbitrary photo-patterning in liquid crystal alignments using DMD based lithography system,” *Opt. Express* **20**, 16684–16689 (2012).
- T. H. Ware, M. E. McConney, J. J. Wie, V. P. Tondiglia, and T. J. White, “Voxelated liquid crystal elastomers,” *Science* **347**, 982–984 (2015).
- S. Palagi, A. G. Mark, S. Y. Reigh, K. Melde, T. Qiu, H. Zeng, C. Parmeggiani, D. Martella, A. Sanchez-Castillo, N. Kapernaum, F. Gisesselmann, D. S. Wiersma, E. Lauga, and P. Fischer, “Structured light enables biomimetic swimming and versatile locomotion of photoresponsive soft microrobots,” *Nat. Mater.* **15**, 647–653 (2016).
- L. De Sio, D. E. Roberts, Z. Liao, S. Nersisyan, O. Uskova, L. Wickboldt, N. Tabiryan, D. M. Steeves, and B. R. Kimball, “Digital polarization holography advancing geometrical phase optics,” *Opt. Express* **24**, 18297–18306 (2016).
- G. F. Walsh, L. De Sio, D. E. Roberts, N. Tabiryan, F. J. Aranda, and B. R. Kimball, “Parallel sorting of orbital and spin angular momenta of light in a record large number of channels,” *Opt. Lett.* **43**, 2256–2259 (2018).
- L. De Sio, D. E. Roberts, Z. Liao, J. Hwang, N. Tabiryan, D. M. Steeves, and B. R. Kimball, “Beam shaping diffractive wave plates,” *Appl. Opt.* **57**, A118–A121 (2018).
- K. Hisano, Y. Kurata, M. Aizawa, M. Ishizu, T. Sasaki, and A. Shishido, “Alignment layer-free molecular ordering induced by masked photopolymerization with non-polarized light,” *Appl. Phys. Express* **9**, 072601 (2016).
- K. Hisano, M. Aizawa, M. Ishizu, Y. Kurata, W. Nakano, N. Akamatsu, C. J. Barrett, and A. Shishido, “Scanning wave photopolymerization enables dye-free alignment patterning of liquid crystals,” *Sci. Adv.* **3**, e1701610 (2017).
- M. Aizawa, K. Hisano, M. Ishizu, N. Akamatsu, C. J. Barrett, and A. Shishido, “Unpolarized light-induced alignment of azobenzene by scanning wave photopolymerization,” *Polym. J.* **50**, 753–759 (2018).